Petroleum Science (2018) 15:709–721
https://doi.org/10.1007/s12182-018-0262-x

ORIGINAL PAPER

Controls on the organic carbon content of the lower Cambrian black shale in the southeastern margin of Upper Yangtze

Yu-Ying Zhang[1] · Zhi-Liang He[2] · Shu Jiang[3] · Shuang-Fang Lu[1] · Dian-Shi Xiao[1] · Guo-Hui Chen[1] · Jian-Hua Zhao[1]

Received: 20 November 2017 / Published online: 13 October 2018

Abstract

Control of various factors, including mineral components, primary productivity and redox level, on the total organic carbon (TOC) in the lower Cambrian black shale from southeastern margin of Upper Yangtze (Taozichong, Longbizui and Yanbei areas) is discussed in detail in this article. Mineral components in the study strata are dominated by quartz and clay minerals. Quartz in the Niutitang Formation is mainly of biogenic origin, and the content is in positive correlation with TOC, while the content of clay minerals is negatively correlated with TOC. Primary productivity, represented by the content of Mo_{bio} (biogenic molybdenum), Ba_{bio} (biogenic barium) and phosphorus, is positively correlated with TOC. The main alkanes in studied samples are nC_{18}–nC_{25}, and odd–even priority values are closed to 1 (0.73–1.13), which suggest the organic matter source was marine plankton. Element content ratios of U/Th and Ni/Co and compound ratio Pr/Ph indicate dysoxic–anoxic bottom water, with weak positive relative with TOC. In total, three main points can be drawn to explain the relationship between data and the factors affecting organic accumulation: (1) quartz-rich and clay-mineral-poor deep shelf–slope–basin environment was favorable for living organisms; (2) high productivity provided the material foundation for organic generation; (3) the redox conditions impact slightly on the content of organic matter under high productivity and dysoxic–anoxic condition.

Keywords Upper Yangtze · Lower Cambrian · Black shale · Total organic carbon

1 Introduction

The early Cambrian recorded substantial changes in global ocean geochemical conditions and biological features compared with late Ediacaran (Knoll and Carroll 1999; Kimura and Watanabe 2001; Wille et al. 2008): a rapid large-scale transgression occurred during the early Cambrian resulted in the global ocean transforming to an anoxic environment from an oxic environment in the late Ediacaran (Fike et al. 2006; Jiang et al. 2009; Babcock et al. 2015); a biological event known as the 'Cambrian Explosion' happened represented by the abundance and species of fossils increasing abruptly (Brasier 1992; Marshall 2006). Based on the geochemical data, the early Cambrian ocean in the Upper Yangtze was strongly stratified and stagnant, with euxinic bottom water (Pi et al. 2013; Feng et al. 2014; Jin et al. 2016) and multiple periods of hydrothermal activities in local areas (Steiner et al. 2001; Pašava et al. 2008; Li et al. 2015).

The lower Cambrian black shale (LCBS) has generally been considered as depositing in an anoxic–euxinic environment in the early Cambrian global transgression (Guo et al. 2007; Lehmann et al. 2007; Liu et al. 2016a, b; Zhang et al. 2017a, b) and it is a high-quality source rock (Hu et al. 2015; Song et al. 2015; Wu et al. 2016; Liu et al.

Edited by Jie Hao

✉ Shu Jiang
sjiang@egi.utah.edu

✉ Shuang-Fang Lu
lushuangfang@upc.edu.cn

Yu-Ying Zhang
yycug@163.com

[1] School of Geosciences, China University of Petroleum (East China), Qingdao 266580, China

[2] Petroleum Exploration and Production Research Institute, SINOPEC, Beijing 100083, China

[3] Energy and Geoscience Institute, University of Utah, Salt Lake City, UT 84102, USA

2017a, b; Zhang et al. 2018) similar to typical black shale in North America, characterized by wide distribution, large thickness (100–400 m), high TOC (2%–10%), which means LCBS has geological advantages for shale gas accumulation (Dong et al. 2009; Liu et al. 2009; Wang et al. 2009a, b; Xiao et al. 2015; Zhang et al. 2015). The LCBS in Upper Yangtze has been well analyzed, focusing on sedimentary environment assessment (Zhu et al. 2003, 2006; Wang et al. 2015a), redox conditions (Guo et al. 2007; Lehmann et al. 2007; Jiang et al. 2009; Wang et al. 2012, 2015b; Xu et al. 2012; Och et al. 2013) and hydrothermal activity (Lott et al. 1999; Steiner et al. 2001; Jiang et al. 2006, 2007; Chen et al. 2009). However, the controlling factors of TOC in the LCBS are still unclear, especially the control from multiple conditions in the sedimentary process.

The southeastern margin of the Upper Yangtze (SMUY) is a promising area in shale gas exploration. This was the important depositional center of black shale during the early Cambrian, with thicker black shale deposited (80–120 m) and larger TOC values (1.5%–20%) than other regions. This study selected three locations (Taozichong, Longbizui and Yanbei) in SMUY, located in deep shelf, slope and deep basin environments, respectively, in the early Cambrian (see locations in Fig. 1).

Furthermore, black shale samples in the lower Cambrian were collected from these 3 locations for geochemical tests to reveal the relationship between geochemical data and TOC. Confirming controlling factors of TOC could provide important theoretical and practical significance for shale gas exploration.

2 Geological setting

The South China Platform was formed by the collision of Yangtze Platform and Cathaysia Platform during the early Neoproterozoic Sibao Orogeny (ca. 1.0 Ga) (Li et al. 2002). Then the South China Platform evolved from a rift basin into a passive continental margin basin at ca. 750 Ma–690 Ma, when it separated from the Rodinia supercontinent during its breakup (Li et al. 1995; Wang and Li 2003).

The Upper Yangtze changed into a deep muddy shelf system in the early Cambrian from a carbonate platform in late Neoproterozoic as a result of large-scale transgression, which could be divided, from west to east, into six sedimentary facies: (1) platform, (2) extension zone, (3) shallow shelf, (4) deep shelf, (5) slope, (6) deep basin (Zhu et al. 2003; Liu et al. 2013, 2016a, b, 2017a, b) (Fig. 1a). At the beginning of the early Cambrian, the relative sea level in the Yangtze Platform was low with high energy, so anoxic water infiltrated to the euphotic zone during transgression. In this stage, it deposited black chert and black siliceous shale in SMUY under the influence of two short periods of siliceous hydrothermal activities (Fig. 1b). During the early Niutitang Stage, the Upper Yangtze became quiet and stratified, when the relative sea level reached its maximum flooding surface, and the chemocline migrated to the euphotic zone. Afterward to the end of the Niutitang Stage, the reducing conditions in the bottom water weakened due to the sea-level falling, while sulfuration appeared in the deep basin only (Xu et al. 2012; Li et al. 2015; Wang et al. 2015b). At the end of the early Cambrian, black shale deposited only in SMUY when the main part of the Upper Yangtze changed to a carbonate platform.

Taozichong area located in Guizhou Province was in a deep shelf environment during the early Cambrian (Fig. 1a); the lower Cambrian strata (overlying the Dengying Formation dolomite unconformably on top of the Ediacaran) are divided into the Taozichong and Niutitang Formations (Fig. 1b). Taozichong Formation is composed of phosphorite (2 m) at the bottom, phosphorous and dolomitic cherts intercalated with thin biological phosphorite with abundant algae microfossils and small shell fossils (Fig. 2a). There was Qingzhen Fauna, consisted of hyoliths, analogous Ediacaran Fauna, Monoplacophora, bradoriid and sponges, found in argillaceous siltstone and silty mudstone upon the siliceous phosphorite (Yang et al. 2002). The lower member of the Niutitang Formation is composed of black siliceous shale (42 m), with simple trace fossils and sponge spicules on the bottom. The upper member of the Niutitang Formation is composed of black carbonaceous shale, dark-gray shale containing trilobites, and siltstone (Fig. 2a).

Longbizui area, located in Hunan Province, was in a slope environment in the early Cambrian (Fig. 1a); the lower Cambrian strata (overlying the Doushantuo Formation conformably) are divided into the Liuchapo and Niutitang Formations (Fig. 1b). The Liuchapo Formation is composed of dark-gray thin-medium chert intercalated by thin siliceous shale.

The lower member of the Niutitang Formation is composed of phosphoric siliceous shale with phosphorite interlayers. The upper member of the Niutitang Formation is composed of thick black carbonaceous shale and mudstone (Fig. 2b). Fossils are rare in the Liuchapo Formation and the lower member of the Niutitang Formation, but sponges and sponge spicules which possibly belong to the *Protospongiidae* sp are common in the upper member of the Niutitang Formation (Wang et al. 2012) (Fig. 2b).

Yanbei area, located in Hunan Province, was in a deep basin environment in the early Cambrian (Fig. 1a); the lower Cambrian strata (overlying the Doushantuo Formation conformably) are divided into the Liuchapo and

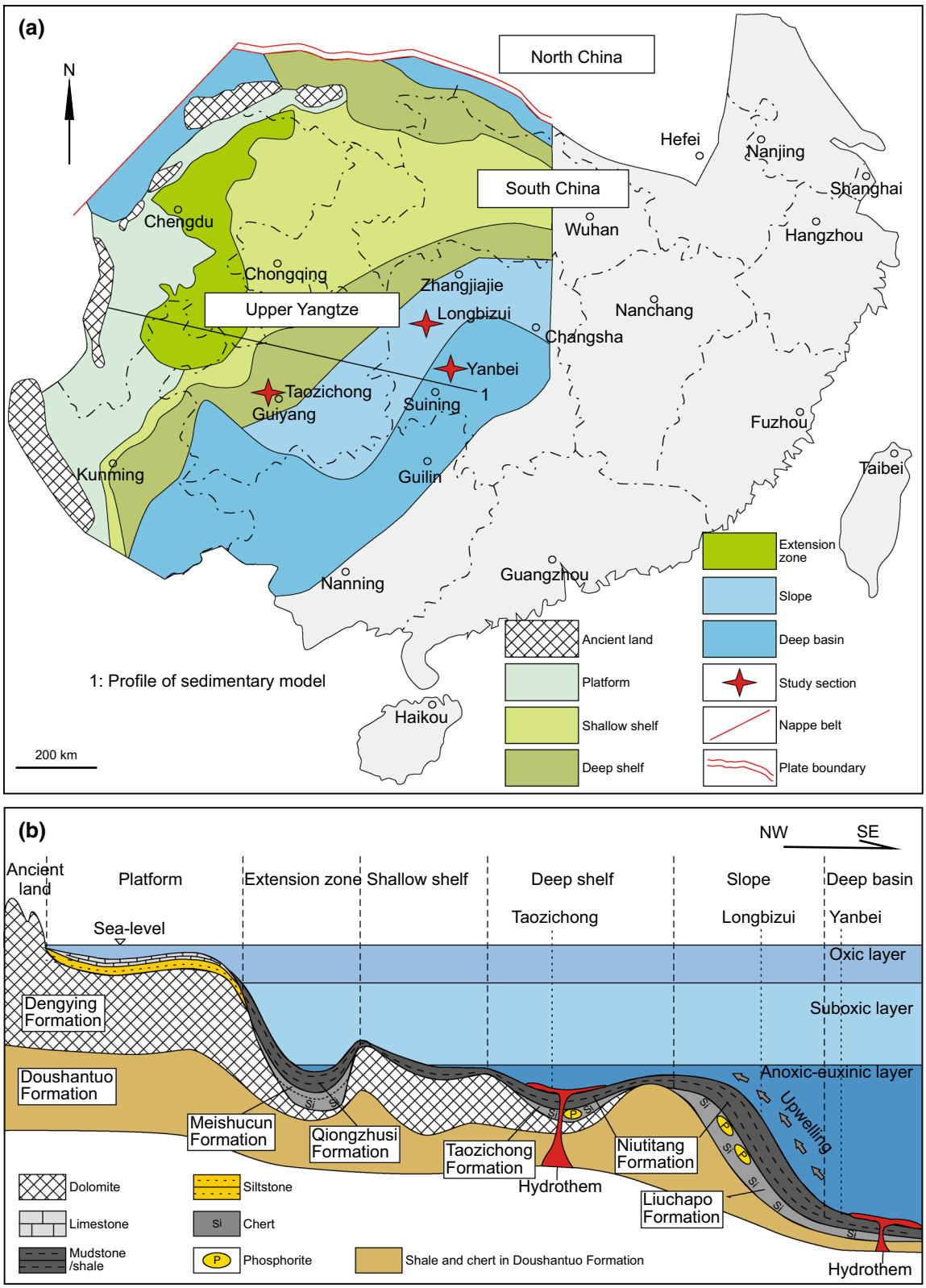

Fig. 1 **a** Lithofacies paleogeographic map in Upper Yangtze during the early Cambrian, from Steiner et al. (2001) and Luo (2014); **b** profile of sedimentary model of lower Cambrian in Upper Yangtze from Pašava et al. (2008)

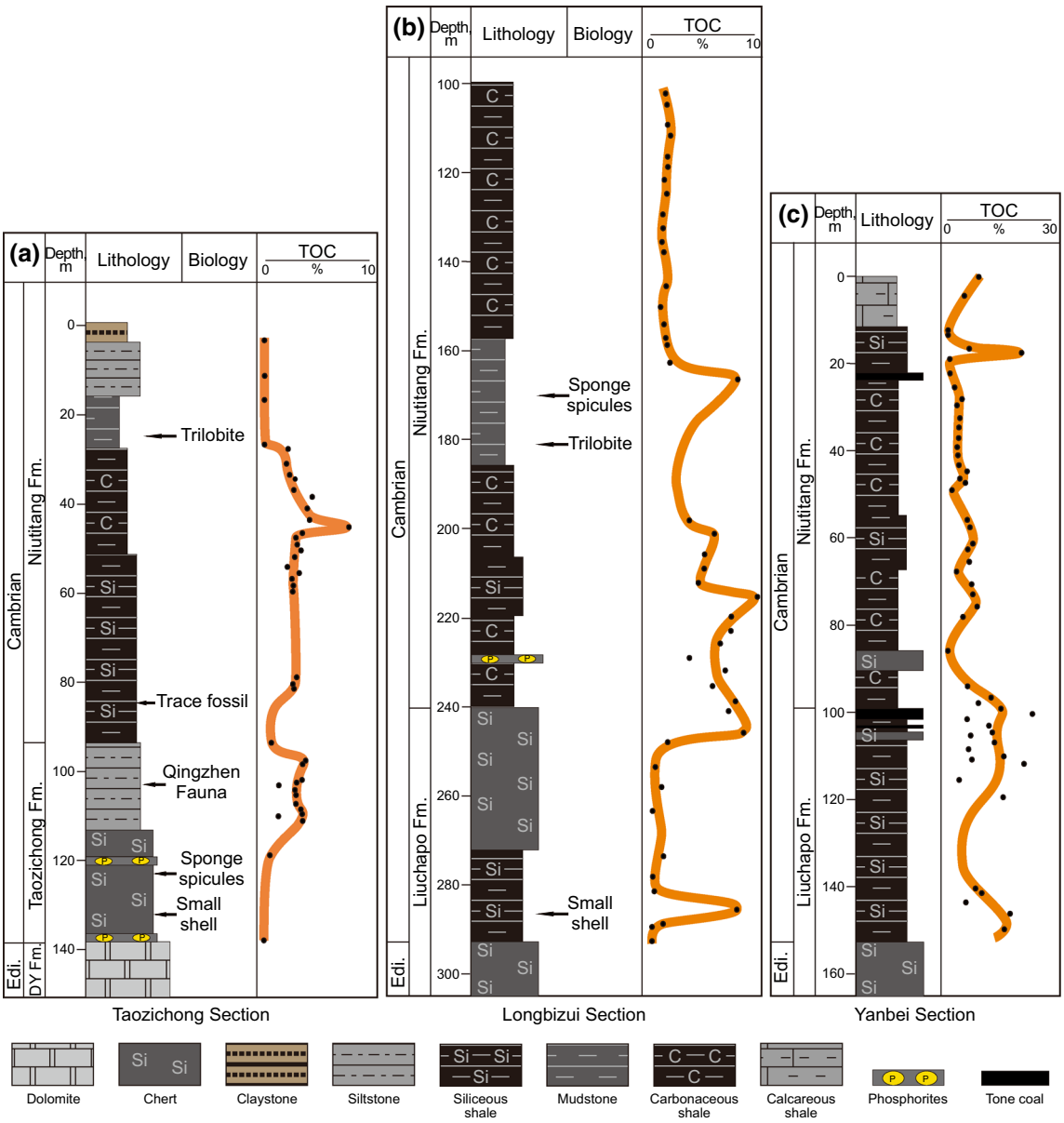

Fig. 2 Stratigraphic column and variation trends of TOC for lower Cambrian black shale in research sections (Fm.: Formation; Edi.: Ediacaran; DY Fm.: Dengying Formation)

Niutitang Formations (Fig. 1b). The Liuchapo Formation is composed of black chert, siliceous shale and carbonaceous shale. The lower member of the Niutitang Formation is composed of black carbonaceous shale, with some chert layers occurring at the base. The upper member of the Niutitang Formation is composed of dark-gray carbonaceous shale and mudstone intercalated by black coal beds, and gray marl at the top (Fig. 2c). Benthic fossils are rare, indicating a deep basin environment in the early Cambrian.

3 Materials and methods

We studied the LCBS from three locations introduced above in SMUY. The fresh rock samples were ground into powders to test TOC (total of 140 samples), mineral components (total of 47 samples), element contents (total of 30 samples) and molecular biomarkers. TOCs were analyzed with a CS-200 Carbon Sulfur Analyzer, and mineral components were examined with a D8 ADVANCE XRD Diffractometer, at the Key Laboratory of Hydrocarbon Accumulation, SINOPEC. The mineral components are presented in Table 1, and TOC results are shown in Fig. 2.

Table 1 Mineral components from XRD

Location	Depth, m	Sample	Clay minerals, %	Quartz, %	Location	Depth, m	Sample	Clay minerals, %	Quartz, %
Taozichong	111.38	TZC-2	41	44	Longbizui	145.64	LBZ-43	37	50
Taozichong	107.75	TZC-4-1	40	36	Longbizui	129.42	LBZ-47	45	41
Taozichong	103.49	TZC-6	41	48	Longbizui	116.29	LBZ-51	43	41
Taozichong	102.42	TZC-7-1	41	37	Longbizui	104.71	LBZ-54	39	41
Taozichong	98.16	TZC-8-1	45	38	Yanbei	143.31	YB-6	28	64
Taozichong	81.46	TZC-10	34	47	Yanbei	137.66	YB-9	29	59
Taozichong	67.27	TZC-13	36	40	Yanbei	109.6	YB-12	45	32
Taozichong	64.67	TZC-15	37	41	Yanbei	106.44	YB-15	36	43
Taozichong	62.67	TZC-17	36	38	Yanbei	102.6	YB-18	27	58
Taozichong	57.11	TZC-21	40	34	Yanbei	95.98	YB-23	7	86
Taozichong	50.85	TZC-25	37	35	Yanbei	74.44	YB-30	17	76
Taozichong	46.8	TZC-28	49	33	Yanbei	64.32	YB-34	14	63
Taozichong	41.36	TZC-31	57	31	Yanbei	60.16	YB-36	16	74
Taozichong	33.86	TZC-35	41	40	Yanbei	54.99	YB-38	17	76
Taozichong	17	TZC-39	40	42	Yanbei	46.71	YB-40	17	71
Longbizui	288.67	LBZ-11	7	85	Yanbei	44.13	YB-42	23	61
Longbizui	278.22	LBZ-14	8	76	Yanbei	34.26	YB-47	24	66
Longbizui	253.59	LBZ-19	7	85	Yanbei	29.24	YB-49	23	67
Longbizui	238.82	LBZ-23	21	54	Yanbei	22.06	YB-52	27	67
Longbizui	225.93	LBZ-27	14	65	Yanbei	17.29	YB-54	12	82
Longbizui	205.85	LBZ-33	27	53	Yanbei	13.24	YB-56	33	59
Longbizui	198.13	LBZ-35	28	49	Yanbei	4.49	YB-60	28	64
Longbizui	166.48	LBZ-37	20	68	Yanbei	0.08	YB-62	15	80
Longbizui	157.22	LBZ-40	38	49					

Element contents were analyzed by X-ray fluorescence (major elements) and inductively coupled plasma mass spectrometry (ICP-MS) (trace elements) at the laboratory of Beijing Research Institute of Uranium Geology, CNNC (China National Nuclear Corporation). Saturated hydrocarbon gas was analyzed by gas chromatography based on standard GB/T 18340.5-2010 at the Key Laboratory of Hydrocarbon Accumulation, SINOPEC (Table 2).

Eu/Eu*, representing Eu enrichment anomaly, was calculated as suggested by Dulski (1994):

$$\mathrm{Eu/Eu^*} = (3 \times \mathrm{Eu_N})/(2 \times \mathrm{Sm_N} + \mathrm{Tb_N})$$

Table 2 Geochemical parameters of saturated hydrocarbons in the Niutitang Formation

Sample	Location	Depth, m	Main alkane	OEP	Pr/Ph
TZC-6	Taozichong	103.49	C_{25}	1.13	0.44
TZC-28	Taozichong	46.8	C_{23}	1.12	0.18
LBZ-23	Longbizui	238.82	C_{23}	1.08	0.44
YB-18	Yanbei	102.6	C_{18}	0.73	0.63

where X_N refers to normalized concentration against PAAS (post-Archean Australian shale) (Taylor and McLennan 1985). The results of Eu/Eu* are presented in Table 3.

Only biogenic elements can indicate primary productivity (Brumsack 2006), so the content of terrigenous elements should be deducted when calculating primary productivity using geochemical elements. Much previous research shows that aluminum (Al) can be used to represent the terrigenous constituent, since Al in silicate minerals is largely immobile during diagenesis as a main component of crustal rocks (Saito et al. 1992). Mo_{bio} and Ba_{bio}, representing biogenetic origin molybdenum and barium, respectively, have been calculated in the formula:

$$w(X_{\mathrm{bio}}) = w(X_{\mathrm{sample}}) - w(\mathrm{Al_{sample}}) \times [w(X)/w(\mathrm{Al})]_{\mathrm{N}}$$

where $w(X_{bio})$ represents the mass fraction of biogenic element X; $w(X_{sample})$ represents mass fraction of element X in sample; $[w(X)/w(Al)]_N$ represents mass fraction of X and Al in PAAS. The results of Mo_{bio} and Ba_{bio} are presented in Table 3.

Table 3 Calculated results of geochemical proxies

Location	Formation	Sample	Depth, m	Ba_{bio}, ppm	Mo_{bio}, ppm	P, %	Ni/Co	U/Th	Eu/Eu^*
Taozichong	Taozichong Formation	TZC-2	111.38	427.32	2.06	0.647	10.52	0.92	1.21
Taozichong	Taozichong Formation	TZC-6	103.49	22.00	4.26	0.081	7.96	1.83	1.09
Longbizui	Niutitang Formation	TZC-8-1	98.16	439.65	99.43	0.177	31.04	1.53	0.82
		TZC-21	57.11	65.17	52.55	0.247	5.64	1.60	1.04
	Niutitang Formation	TZC-25	50.85	183.59	96.50	0.293	10.35	2.61	1.07
	Liuchapo Formation	TZC-28	46.8	385.12	170.55	0.319	7.71	2.36	1.01
		TZC-33	37.23	501.44	46.85	0.263	4.27	2.66	1.12
		TZC-37	28	444.65	44.08	0.175	5.68	1.18	1.01
		TZC-41	3.5	0.00	0.00	0.139	5.02	0.29	1.04
		LBZ-11	288.67	452.16	0.11	0.023	16.22	6.54	1.16
Longbizui	Liuchapo Formation	LBZ-13	281.35	9898.51	2.02	0.04	27.27	3.05	0.52
Yanbei	Niutitang Formation	LBZ-14	278.22	1276.17	0.12	0.023	5.98	1.98	0.66
		LBZ-22	240.92	4177.66	0.36	0.091	18.29	15.48	1.16
		LBZ-26	229.02	23,064.73	1.42	0.218	16.45	6.39	0.29
	Niutitang Formation	LBZ-31	212.03	14,506.03	1.93	0.062	11.27	2.75	0.63
	Liuchapo Formation	LBZ-40	157.22	3265.33	2.39	0.079	8.68	0.63	0.88
		LBZ-44	137.92	2807.70	2.53	0.06	7.04	0.63	0.94
		LBZ-47	129.42	3096.87	2.69	0.049	10.40	0.46	0.86
		LBZ-51	116.29	2292.88	2.80	0.077	4.10	0.54	0.87
		LBZ-54	104.71	1769.55	2.55	0.082	4.54	0.44	0.89
		YB-6	143.31	3661.34	33.36	0.124	39.45	4.98	1.05
Yanbei	Liuchapo Formation	YB-9	137.66	10,750.06	64.93	0.032	7.20	3.53	0.59
	Niutitang Formation	YB-14	107.98	2471.04	20.13	0.071	15.34	9.49	0.92
		YB-18	102.6	6586.21	138.77	0.259	11.66	7.92	1.05
		YB-20	99.67	1720.12	43.81	0.036	8.11	1.61	1.09
		YB-35	61.71	1304.88	60.70	0.067	4.45	3.02	1.00
	Niutitang Formation	YB-40	46.71	926.42	43.94	0.034	6.35	1.54	0.98
		YB-45	38.56	1391.91	15.75	0.018	4.08	0.63	0.91
		YB-52	22.06	2795.35	44.82	0.024	16.17	4.29	0.73
		YB-56	13.24	3478.19	419.06	0.068	20.38	2.69	0.93

4 Results and discussion

4.1 Relationship between TOC and mineral components

Mineral components of the lower Cambrian strata in SMUY are dominated by quartz, followed by clay minerals, with a little feldspar, carbonate, pyrite and anhydrite (Table 1). The SMUY was located in a deep shelf–deep basin environment during the early Cambrian (Steiner et al. 2001; Zhu et al. 2003) far from the western ancient land (Fig. 1), where the depositional interface was under wave base or storm-wave base. Therefore, clay minerals deposited through a long transportation by wind and waves, in this case the content of clay minerals was mainly controlled by offshore distance. Europium (Eu) shows a positive anomaly generally in oceanic hydrothermal deposition (Ruhlin and Owen 1986; Douville et al. 1999), in which $Eu/Eu^* > 1$ represents a positive anomaly. The formula for Eu/Eu^* is discussed in Sect. 3.

The SMUY experienced multi-period hydrothermal activities in the early Cambrian, resulting in $Eu/Eu^* > 1$ for all the samples from Taozichong (except TZC-8-1 and TZC-13), and most of the samples in the Liuchapo Formation from Longbizui and Yanbei (Table 3). The quartz in the strata affected by hydrothermal activities was hydrothermal origin without any obvious linear relation with TOC. Therefore, the relationship between TOC and the content either of biogenic quartz or of clay minerals in the samples from the Niutitang Formation in Longbizui and Yanbei would be discussed mainly in this article. The microlitic quartz in black shale was derived mainly from

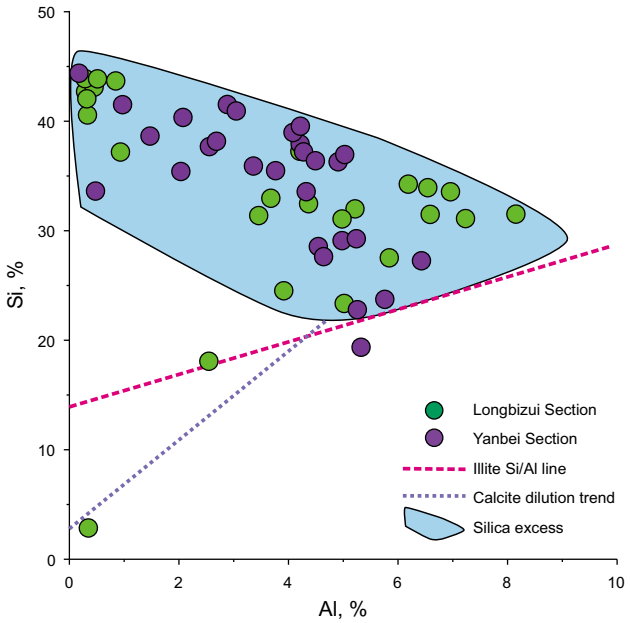

Fig. 3 Cross-plot of Si and Al contents in lower Cambrian shale

the opals in sponge spicules and radiolarians (Bowker 2003), the content of which was far more than the terrestrial quartz in such as Niutitang black siliceous shale (Loucks and Ruppel 2007). As suggested by Rowe et al. (2008), ratios of Si/Al located above Si/Al in illite (fitted by contents of Si and Al in the Barnett shale) represent biogenic excess Si contained in shale. The majority of Si/Al in the Niutitang Formation has been located in silica excess region, which means biogenic quartz dominated in the Niutitang shale (Fig. 3). It shows an obvious positive relation between TOC and content of quartz (Fig. 4a, c) and an obvious negative relation between TOC and content of clay minerals in the Niutitang shale from these two locations (Fig. 4b, d). That is to say, more quartz and less clay minerals accompany higher TOC (Fig. 5). Because more quartz represents larger biomass in the Niutitang shale, the deep shelf and deep basin environments, quartz-rich and clay-mineral-poor, provided a favorable living environment for marine organisms (i.e., bacteria, algae, radiolarian, sponge, bradoriid and eodiscid). In general, the TOC is positively correlated with the content of quartz and

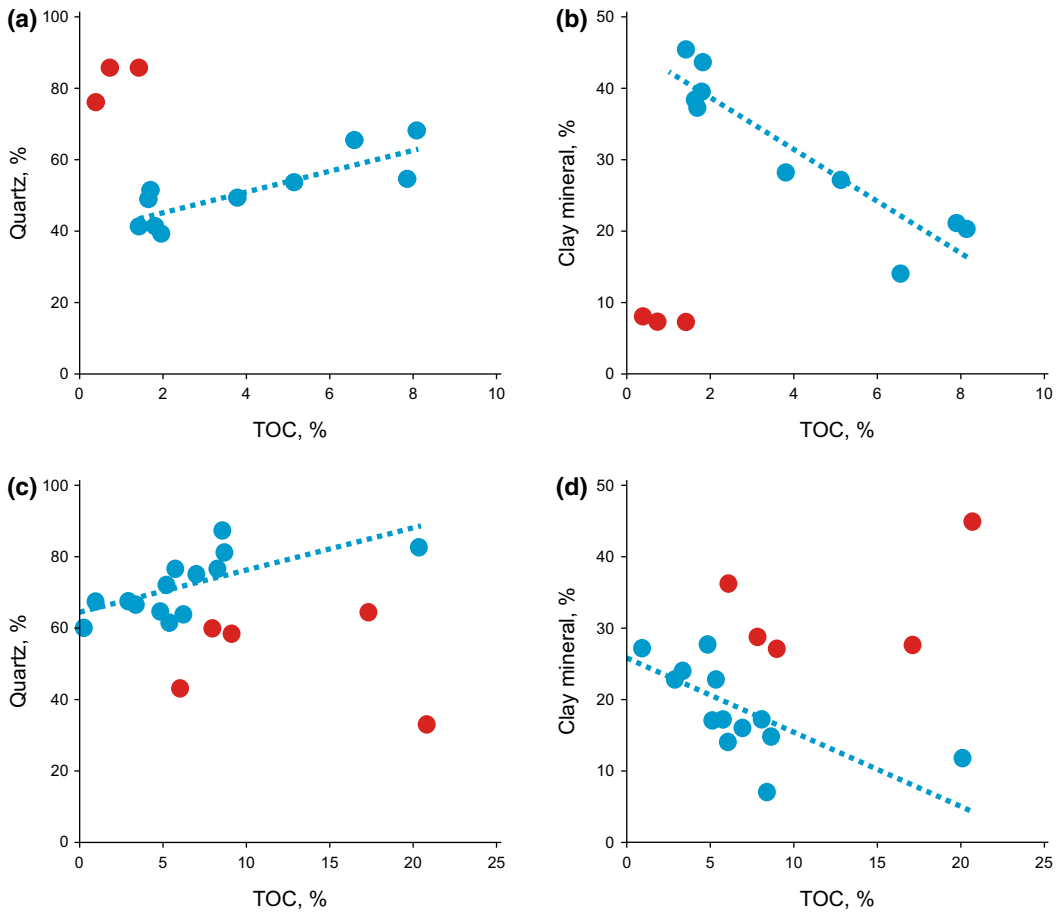

Fig. 4 Correlation diagram between TOC and mineral components (**a**, **b** Longbizui; **c**, **d** Yanbei. Red points are from the Liuchapo Formation, blue points are from the Niutitang Formation. Dotted lines represent trend lines)

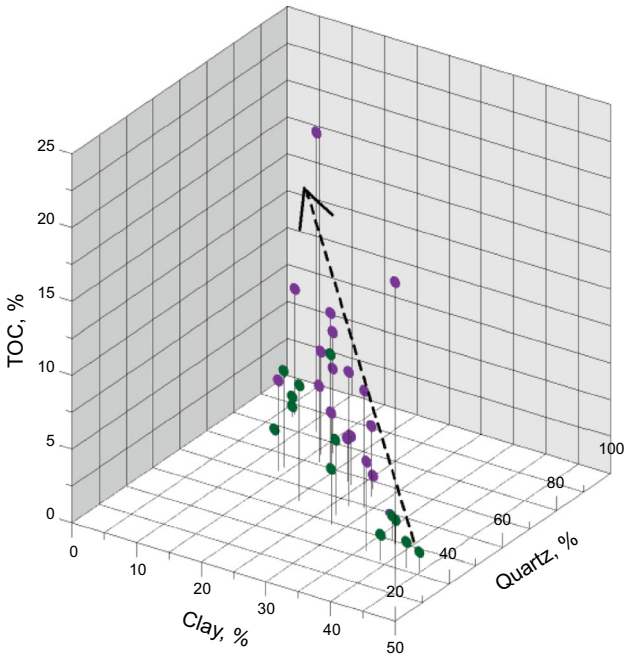

Fig. 5 Correlation diagram between TOC and the content of quartz and clay minerals (green points are from Longbizui; purple points are from Yanbei. The arrow line represents the trend)

negatively correlated with the content of clay minerals, thus the deep shelf–deep basin environment favored the enrichment of organic matter.

4.2 Relationship between TOC and primary productivity

Primary productivity is the velocity of energy fixation by paleo-marine organisms during the energy cycle, i.e., the amount of organic matter generation per unit area and per unit time. Previous research shows that molybdenum (Mo) deposits in the form of stable sulfide through combination of $Mo(O_x, S_{4-x})^{2-}$ (x = 0–3) and sulfur-rich organic molecules (Tribovillard et al. 2004) or/and pyrites (Vorlicek et al. 2004) under anoxic conditions with participation of organic matter. This kind of combination is irreversible (Bostick et al. 2003), which would lead to more Mo deposited with more organic carbon availability. In bathyal–abyssal regions where primary productivity is high, both the barium (Ba) flux in sea water and the content of barite in deposition are high, with a 30% preserving rate of biologic Ba (Dymond et al. 1992; Paytan et al. 1996), thus the relationship between Ba and primary productivity in surface water could be established (Francois et al. 1995). The calculating formula of Mo_{bio} and Ba_{bio} is discussed in Sect. 3. As a crucial nutrient element (Howarth 1988), phosphorus (P) in deposits is contained in dead plankton falling on the water–sediment interface; for this reason, the content of P can reflect primary productivity largely in geological epochs (Tyrrell 1999). In general, low molecular weight *n*-alkanes were sourced from plankton, algae or bacteria, while high molecular weight n-alkanes were source from advanced plants (Clark and Blumer 1967).

It shows an obvious positive relationship between TOC and Mo_{bio}, Ba_{bio} and P in the samples from Taozichong and Longbizui (Fig. 6). Likewise, it shows an obvious positive relationship between TOC and Mo_{bio} and P in the samples from Yanbei (Fig. 6g, i); however, the relationship between TOC and Ba_{bio} in this location shows a weaker relationship than the other two locations (Fig. 6h). It is because the Yanbei area was located in a deep basin environment during the early Cambrian which was deeper than the other two areas with sulfide bottom water containing free H_2S. In this case, sulfate could be reduced by sulfur-reducing bacteria resulting in the $BaSO_4$ crystals dissolving (Dymond et al. 1992), which could weaken the relativity between TOC and Ba_{bio} in Yanbei. As it shows an obvious positive relationship between TOC and primary productivity in the LCBS from these three locations, primary productivity could provide the basis for organic accumulations in black shale (Pedersen and Calvert 1990), and organic carbon formed by primary productivity could still remain after a series of complex processes, e.g., deposition and burial. Alkane distribution in studied samples are nC_{18}–nC_{25}, and odd–even priority (OEP) values are close to 1 (0.73–1.13) (Table 2), which suggest organic matter was from marine plankton, e.g., algae and bacteria.

4.3 Relationship between TOC and redox conditions

Pristane (Pr) and phytane (Ph) can be used as paleo-redox indicator: Ph has obvious advantage in a (strong) anoxic depositional environment, while Pr abundance is advantaged in a weak anoxic or oxic environment (Peters and Moldowan 1991). The ratios of trace metals, such as U/Th and Ni/Co, can be used to evaluate redox conditions. Uranium (U) usually dissolves in oxic seawater as U^{6+}, while it could be absorbed easily by organic particles as U^{4+} in anoxic seawater (Algeo and Maynard 2004). In contrast to the U, thorium (Th) is concentrated in weathering-resistant minerals as a constituent of heavy minerals and clay minerals. Th does not migrate easily in a low-temperature environment. Therefore, ratios of U/Th can represent redox conditions in seawater, as Jones and Manning (1994) suggested that U/Th < 0.75 indicates oxic conditions, $0.75 <$ U/Th < 1.25 indicates dysoxic conditions, U/Th > 1.25 indicates anoxic conditions. Nickel (Ni) and cobalt (Co) usually exist in pyrite, and a higher ratio of Ni/Co indicates stronger reducing conditions. Jones and Manning (1994) suggested that Ni/Co < 5 indicates oxic

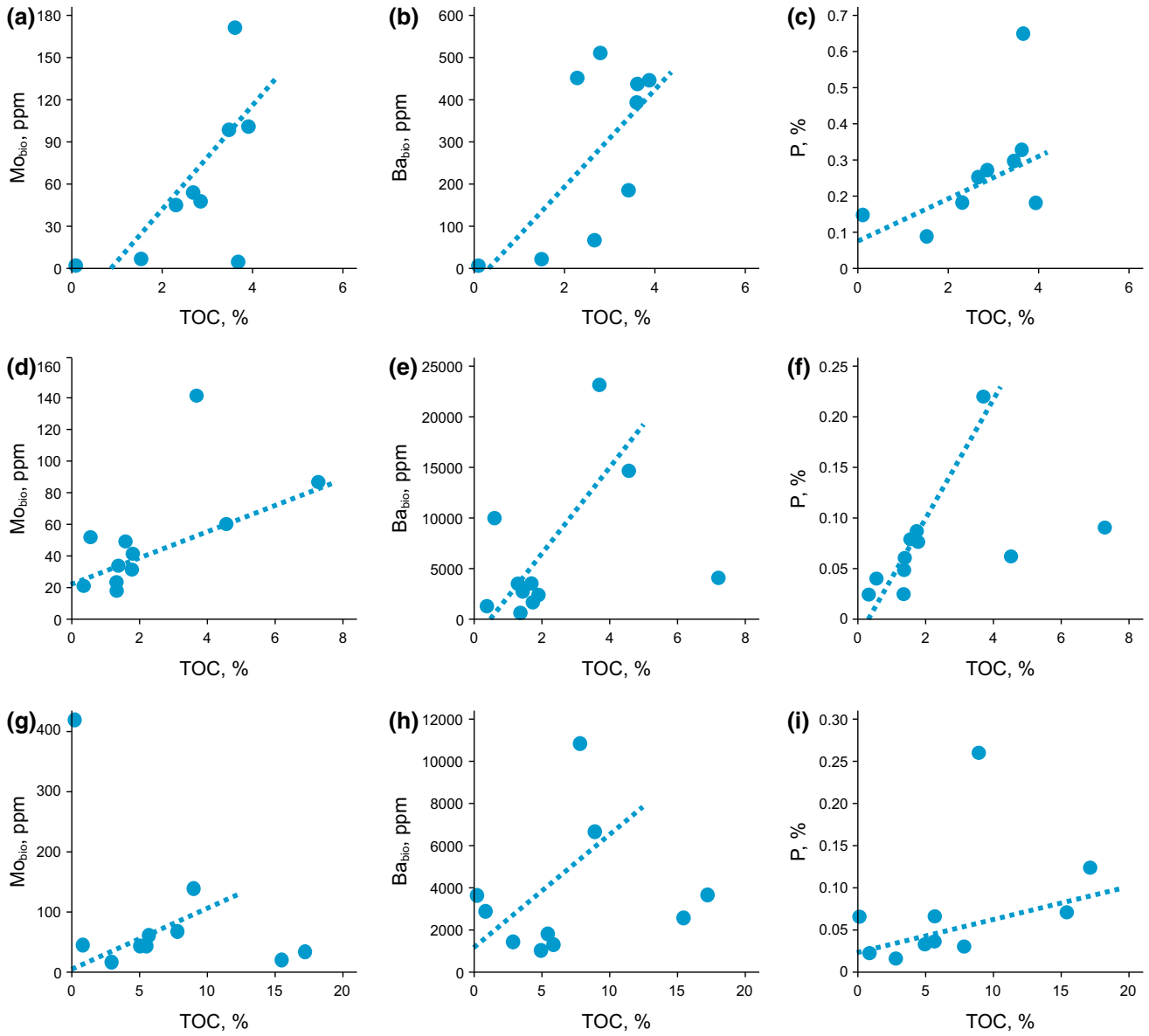

Fig. 6 Correlation diagram between TOC and indicators of primary productivity (**a**, **b**, **c** Taozichong; **d**, **e**, **f** Longbizui; **g**, **h**, **i** Yanbei. Dotted lines represent correlation trends)

Table 4 Statistical table of average TOC and redox level in three locations

Location	Sedimentary environment	U/Th average	Ni/Co average	TOC average, %
Taozichong	Deep shelf	1.66	9.80	2.73
Longbizui	Slope	3.54	11.84	3.40
Yanbei	Deep basin	3.97	13.32	7.26

conditions, $5 < \text{Ni/Co} < 7$ indicates dysoxic conditions, $\text{Ni/Co} > 7$ indicates anoxic conditions.

In this study, Pr/Ph values change from 0.18 to 0.63 (Table 2), indicating strong-normal anoxic environment in LCBS. The average values of U/Th and Ni/Co are 1.66 and 9.80 (Taozichong), 3.54 and 11.84 (Longbizui), 3.97 and 13.32 (Yanbei), respectively, which shows the reducing conditions are Taozichong < Longbizui < Yanbei (Table 4). Almost all of the geochemical parameters show dysoxic and anoxic bottom water covered the sedimentary

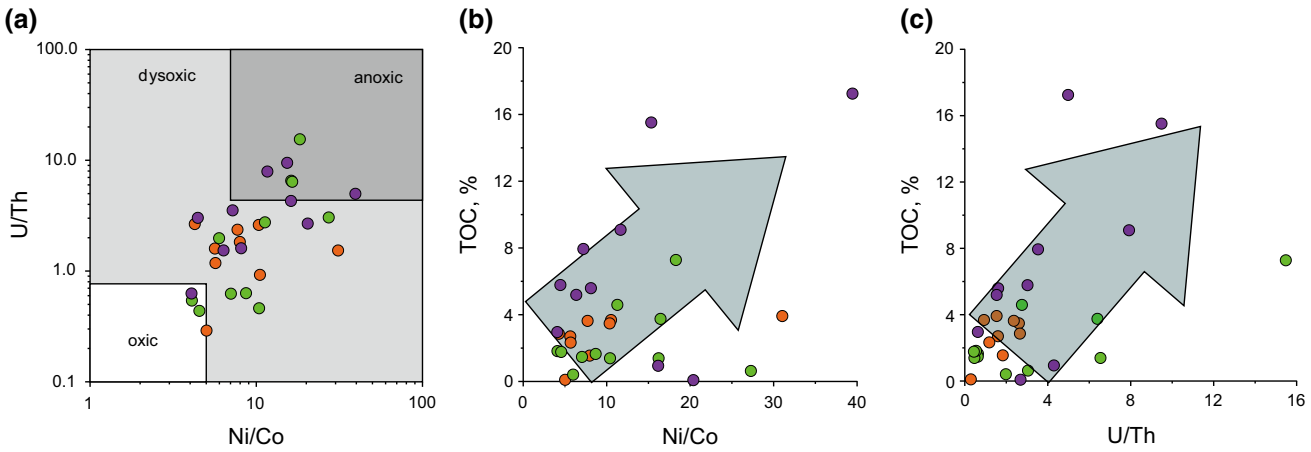

Fig. 7 Correlation diagram between TOC and redox indicators (the ordinate scale is log of 10)

interface of black shale in SMUY (Fig. 7a). Moreover, a weak positive relationship existing between TOC and ratio of U/Th and of Ni/Co can be observed (Fig. 7b, c). In consequence, LCBS deposited under dysoxic–anoxic bottom water, which was beneficial for organic preservation, while the effect of reducing intensity on organic accumulation is quite weak.

4.4 Main factors affecting organic accumulation

The development of marine black shale is caused by multiple factors of sedimentary conditions. In addition, marine black shale would deposit only when each of the factors reaches a favorable condition, rather than emphasizing the influence from just one of them. Normally, organic accumulation needs two main conditions: (1) favorable preservation, which means bottom water should be dysoxic anoxic (Jenkyns 2010; Sun et al. 2016); (2) high primary productivity, which means abundant plankton living in surface water (Pedersen and Calvert 1990).

During the early Cambrian, the Yangtze Platform was located between 30° and 60° north latitude in the subtropical dry zone controlled by subtropical highs, where broad equatorial current divergence developed in the oceanic bottom, transformed into eutrophic upwelling at the continental margin like SMUY (Xia et al. 2015; Tang et al. 2017; Yeasmin et al. 2017). In consequence, the species and number of organisms in the early Cambrian increased rapidly in quartz-rich and clay-mineral-poor deep shelf–slope–basin environments, resulting in massive quantities of organic matter settling down and being buried, which is represented by high values from geochemical parameters of primary productivity (Mo_{bio}, Ba_{bio} and P) and the obvious positive relationship between these parameters and TOC. On the other hand, the LCBS deposited in dysoxic–anoxic bottom water, which was beneficial for preservation of organic matter generated by productivity in surface water. However, an extremely weak positive relativity between the geochemical parameters of redox (Ni/Co and U/Th) and TOC could be found, which might mean an adequate source of organic matter diminished the importance of organic preservation, especially under dysoxic–anoxic bottom water.

In total, three main points can be drawn to explain the relationship between data and the factors affecting organic accumulation: (1) quartz-rich and clay-mineral-poor deep shelf–slope–basin environments provided a favorable environment for living organisms; (2) high primary productivity provided the foundation for organic matter generation; (3) redox levels impact slightly on the content of organic matter under high productivity and dysoxic–anoxic condition.

5 Conclusions

In conclusion, content of organic matter in the lower Cambrian black shale in SMUY is controlled by the following factors:

(1) Quartz in samples of the Niutitang Formation in Longbizui and Yanbei was of biogenic origin indicated by excess Si content, and there is a positive correlation between the content of quartz and TOC and a negative correlation between the content of clay minerals and TOC. A deep shelf–deep basin environment with abundant marine organisms and featuring quartz-rich and clay-poor lithofacies provided a favorable environment for the living organisms.

(2) Primary productivity in these three locations, represented by contents of Mo_{bio}, Ba_{bio} and P, was positively correlated to TOC in the lower Cambrian

black shale. Organic geochemical data suggest organic matter was sourced from plankton. High primary productivity provided a basis for organic matter generation, and organic carbon formed by primary productivity could survive after a series of complex processes.

(3) Geochemical parameters of redox (Pr/Ph, Ni/Co and U/Th) suggest the lower Cambrian black shale deposited in dysoxic–anoxic bottom water, which was beneficial for preservation of organic matter generated by productivity in surface water. However, the weak positive relativity between the TOC and ratios of Ni/Co and U/Th means redox conditions impact only slightly on the content of organic matter under high productivity and dysoxic–anoxic condition.

Acknowledgements This work is supported by the National Natural Science Foundation Research (Grant 41672130, 41728004), the National Key S&T Special Projects (Grant 2016ZX05061-003-001), the National Postdoctoral Innovative Talent Support Program (Grant BX201700289), China Postdoctoral Science Foundation (Grant 2017M620296). We appreciate SINOPEC providing the samples. We also appreciate Dr. Zhenrui Bai from SINOPEC for polishing this paper.

References

Algeo TJ, Maynard JB. Trace-element behavior and redox facies in core shales of Upper Pennsylvanian Kansas-type cyclothems. Chem Geol. 2004;206(3–4):289–318. https://doi.org/10.1016/j.chemgeo.2003.12.009.

Babcock LE, Peng SC, Brett CE, et al. Global climate, sea level cycles, and biotic events in the Cambrian Period. Palaeoworld. 2015;24(1–2):5–15. https://doi.org/10.1016/j.palwor.2015.03.005.

Brasier MD. Background to the Cambrian explosion. J Geol Soc Lond. 1992;149(4):585–7. https://doi.org/10.1144/gsjgs.149.4.0585.

Bostick BC, Fendorf S, Helz GR. Differential adsorption of molybdate and tetrathiomolybdate on pyrite (FeS_2). Environ Sci Technol. 2003;37(2):285–91. https://doi.org/10.1021/es0257467.

Bowker KA. Recent developments of the Barnett Shale play, Fort Worth Basin. West Tex Geol Soc Bull. 2003;42(6):4–11.

Brumsack HJ. The trace metal content of recent organic carbon-rich sediments: implications for Cretaceous black shale formation. Palaeogeogr Palaeoclimatol Palaeoecol. 2006;232(2):344–61. https://doi.org/10.1016/j.palaeo.2005.05.011.

Chen D, Wang J, Qing H, et al. Hydrothermal venting activities in the early Cambrian, South China: petrological, geochronological and stable isotopic constraints. Chem Geol. 2009;258(3):168–81. https://doi.org/10.1016/j.chemgeo.2008.10.016.

Clark RC, Blumer M. Distribution of *n*-paraffins in marine organisms and sediment. Limnol Oceanogr. 1967;12(1):79–87. https://doi.org/10.4319/lo.1967.12.1.0079.

Dong DZ, Cheng KM, Wang SQ, et al. An evaluation method of shale gas resource and its application in the Sichuan Basin. Nat Gas Ind. 2009;29(5):33–9 **(in Chinese)**.

Douville E, Bienvenu P, Charlou JL, et al. Yttrium and rare earth elements in fluids from various deep-sea hydrothermal systems. Geochim Cosmochim Acta. 1999;63(5):627–43. https://doi.org/10.1016/S0016-7037(99)00024-1.

Dulski P. Interferences of oxide, hydroxide and chloride analyte species in the determination of rare earth elements in geological samples by inductively coupled plasma-mass spectrometry. Fresenius J Anal Chem. 1994;350(4–5):194–203. https://doi.org/10.1007/BF00322470.

Dymond J, Suess E, Lyle M. Barium in deep-sea sediment: a geochemical proxy for paleoproductivity. Paleoceanography. 1992;7(2):163–81. https://doi.org/10.1029/92PA01080.

Feng LJ, Li C, Huang J, et al. A sulfate control on marine mid-depth euxinia on the early Cambrian (ca. 529–521 Ma) Yangtze platform, South China. Precambrian Res. 2014;246(6):123–33. https://doi.org/10.1016/j.precamres.2014.03.002.

Fike DA, Grotzinger JP, Pratt LM, et al. Oxidation of the Ediacaran ocean. Nature. 2006;444(7120):744–7. https://doi.org/10.1038/nature05345.

Francois R, Honjo S, Manganini SJ, et al. Biogenic barium fluxes to the deep sea: implications for paleoproductivity reconstruction. Glob Biogeochem Cycles. 1995;9(2):289–303. https://doi.org/10.1029/95gb00021.

Guo Q, Shields GA, Liu C, et al. Trace element chemostratigraphy of two Ediacaran–Cambrian successions in South China: implications for organosedimentary metal enrichment and silicification in the early Cambrian. Palaeogeogr Palaeoclimatol Palaeoecol. 2007;254(1–2):194–216. https://doi.org/10.1016/j.palaeo.2007.03.016.

Howarth RW. Nutrient limitation of net primary production in marine ecosystems. Annu Rev Ecol Syst. 1988;19(4):89–110. https://doi.org/10.1146/annurev.es.19.110188.000513.

Hu QH, Liu XG, Gao ZY, et al. Pore structure and tracer migration behavior of typical American and Chinese shales. Pet Sci. 2015;12(4):651–63. https://doi.org/10.1007/s12182-015-0051-8.

Jenkyns HC. Geochemistry of oceanic anoxic events. Geochem Geophys Geosyst. 2010;11(3):66–81. https://doi.org/10.1016/j.orggeochem.2016.05.018.

Jiang SY, Chen YQ, Ling HF, et al. Trace- and rare-earth element geochemistry and Pb–Pb dating of black shales and intercalated Ni–Mo–PGE–Au sulfide ores in lower Cambrian strata, Yangtze Platform, South China. Miner Depos. 2006;41(5):453–67. https://doi.org/10.1007/s00126-006-0066-6.

Jiang SY, Yang J, Ling HF, et al. Extreme enrichment of polymetallic Ni–Mo–PGE–Au in lower Cambrian black shales of South China: an Os isotope and PGE geochemical investigation. Palaeogeogr Palaeoclimatol Palaeoecol. 2007;254(2):217–28. https://doi.org/10.1016/j.palaeo.2007.03.024.

Jiang SY, Pi DH, Heubeck C, et al. Early Cambrian ocean anoxia in South China. Nature. 2009;459(7248):E5–6. https://doi.org/10.1038/nature08048.

Jin CS, Li C, Algeo TJ, et al. A highly redox-heterogeneous ocean in South China during the early Cambrian (~ 529–514 Ma): implications for biota-environment co-evolution. Earth Planet Sci Lett. 2016;441:38–51. https://doi.org/10.1016/j.epsl.2016.02.019.

Jones B, Manning DAC. Comparison of geochemical indices used for the interpretation of depositional environments in ancient

mudstones. Chem Geol. 1994;111(1–4):112–29. https://doi.org/10.1016/0009-2541(94)90085-X.

Knoll AH, Carroll SB. Early animal evolution: emerging views from comparative biology and geology. Science. 1999;284(5423):2129–37. https://doi.org/10.1126/science.284.5423.2129.

Kimura H, Watanabe Y. Oceanic anoxia at the Precambrian–Cambrian boundary. Geology. 2001;29(11):995–8. https://doi.org/10.1130/0091-7613(2001)029<0995:OAATPC>2.0.CO;2.

Lehmann B, Nägler TF, Holland HD, et al. Highly metalliferous carbonaceous shale and early Cambrian seawater. Geology. 2007;35(5):403–6. https://doi.org/10.1130/G23543A.1.

Li ZX, Zhang LH, Powell CW. South China in Rodinia: part of the missing link between Australia–East Antarctica and Laurentia? Geology. 1995;23(5):407–10. https://doi.org/10.1130/0091-7613(1995)023<0407:SCIRPO>2.3.CO;2.

Li ZX, Li XH, Zhou H, et al. Grenvillian continental collision in South China: new SHRIMP U–Pb zircon results and implications for the configuration of Rodinia. Geology. 2002;30(2):163–6. https://doi.org/10.1130/0091-7613(2002)030<0163:GCCISC>2.0.CO;2.

Li YF, Fan TL, Zhang JP, et al. Geochemical changes in the early Cambrian interval of the Yangtze Platform, South China: implications for hydrothermal influences and paleocean redox conditions. J Asian Earth Sci. 2015;109:100–23. https://doi.org/10.1016/j.jseaes.2015.05.003.

Liu SG, Zeng XL, Huang WM, et al. Basic characteristics of shale and continuous-discontinuous transition gas reservoirs in Sichuan Basin, China. J Chengdu Univ Technol Sci Technol Ed. 2009;36(6):578–92 **(in Chinese)**.

Liu SG, Sun W, Luo ZL, et al. Xingkai taphrogenesis and petroleum exploration from Upper Sinian to Cambrian Strata in Sichuan Basin, China. J Chengdu Univ Technol Sci Technol Ed. 2013;40(5):511–20. https://doi.org/10.3969/j.issn.1671-9727.2013.05.03.

Liu J, Yao YB, Elsworth D, et al. Sedimentary characteristics of the lower Cambrian Niutitang shale in the southeast margin of Sichuan Basin, China. J Nat Gas Sci Eng. 2016a;36:1140–50. https://doi.org/10.1016/j.jngse.2016.03.085.

Liu SG, Wang YG, Wei S, et al. Control of intracratonic sags on the hydrocarbon accumulations in the marine strata across the Sichuan Basin, China. J Chengdu Univ Technol Sci Technol Ed. 2016b;43(1):1–23. https://doi.org/10.3969/j.issn.1671-9727.2016.01.01.

Liu XP, Jin ZJ, Bai GP, et al. Formation and distribution characteristics of Proterozoic–Lower Paleozoic marine giant oil and gas fields worldwide. Pet Sci. 2017a;14(2):237–60. https://doi.org/10.1007/s12182-017-0154-5.

Liu ZB, Gao B, Zhang YY, et al. Types and distribution of the shale sedimentary facies of the lower Cambrian in Upper Yangtze area, South China. Pet Explor Dev. 2017b;44(1):20–31. https://doi.org/10.1016/S1876-3804(17)30004-6.

Loucks RG, Ruppel SC. Mississippian Barnett Shale: lithofacies and depositional setting of a deep-water shale-gas succession in the Fort Worth Basin, Texas. AAPG Bull. 2007;91(4):579–601. https://doi.org/10.1306/11020606059.

Lott DA, Coveney RMJ, Murowchick JB, et al. Sedimentary exhalative nickel–molybdenum ores in South China. Econ Geol. 1999;94(7):1051–66. https://doi.org/10.2113/gsecongeo.94.7.1051.

Luo C. Geological characteristics of gas shale in the lower Cambrian Niutitang Formation of the Upper Yangtze Platform. Chengdu: Chengdu University of Technology; 2014. p. 115–32 **(in Chinese)**.

Marshall CR. Explaining the Cambrian "explosion" of animals. Annu Rev Earth Planet Sci. 2006;34(34):355–84.

Och LM, Shields-Zhou GA, Poulton SW, et al. Redox changes in early Cambrian black shales at Xiaotan section, Yunnan Province, South China. Precambrian Res. 2013;225(1):166–89. https://doi.org/10.1016/j.precamres.2011.10.005.

Pašava J, Kříbek B, Vymazalová A, et al. Multiple sources of metals of mineralization in lower Cambrian black shales of South China: evidence from geochemical and petrographic study. Resour Geol. 2008;58(1):25–42. https://doi.org/10.1111/j.1751-3928.2007.00042.x.

Paytan A, Moore WS, Kastner M. Sedimentation rate as determined by ^{226}Ra activity in marine barite. Geochim Cosmochim Acta. 1996;60(22):4313–9. https://doi.org/10.1016/S0016-7037(96)00267-0.

Pedersen TF, Calvert SE. Anoxia versus productivity; what controls the formation of organic-carbon-rich sediments and sedimentary rocks? AAPG Bull. 1990;74(4):454–66. https://doi.org/10.1306/0C9B232B-1710-11D7-8645000102C1865D.

Peters KE, Moldowan JM. Effects of source, thermal maturity, and biodegradation on the distribution and isomerization of homohopanes in petroleum. Org Geochem. 1991;17(1):47–61.

Pi DH, Liu CQ, Shields-Zhou GA, et al. Trace and rare earth element geochemistry of black shale and kerogen in the early Cambrian Niutitang Formation in Guizhou Province, South China: constraints for redox environments and origin of metal enrichments. Precambrian Res. 2013;225(1):218–29. https://doi.org/10.1016/j.precamres.2011.07.004.

Rowe HD, Loucks RG, Ruppel SC, et al. Mississippian Barnett Formation, Fort Worth Basin, Texas: bulk geochemical inferences and Mo–TOC constraints on the severity of hydrographic restriction. Chem Geol. 2008;257(1–2):16–25. https://doi.org/10.1016/j.chemgeo.2008.08.006.

Ruhlin DE, Owen RM. The rare earth element geochemistry of hydrothermal sediments from the East Pacific Rise: examination of a seawater scavenging mechanism. Geochim Cosmochim Acta. 1986;50(3):393–400. https://doi.org/10.1016/0016-7037(86)90192-4.

Saito C, Noriki S, Tsunogai S. Particulate flux of A1, a component of land origin, in the western North Pacific. Deep Sea Res Part A Oceanogr Res Pap. 1992;39(7–8):1315–27. https://doi.org/10.1016/0198-0149(92)90071-Z.

Song Y, Li Z, Jiang L, et al. The concept and the accumulation characteristics of unconventional hydrocarbon resources. Pet Sci. 2015;12(4):563–72. https://doi.org/10.1007/s12182-015-0060-7.

Steiner M, Wallis E, Erdtmann B, et al. Submarine-hydrothermal exhalative ore layers in black shales from South China and associated fossils—insights into a lower Cambrian facies and bio-evolution. Palaeogeogr Palaeoclimatol Palaeoecol. 2001;169(3):165–91. https://doi.org/10.1016/S0031-0182(01)00208-5.

Sun X, Zhang TW, Sun YG, et al. Geochemical evidence of organic matter source input and depositional environments in the lower and upper Eagle Ford Formation, south Texas. Org Geochem. 2016;98:66–81. https://doi.org/10.1016/j.orggeochem.2016.05.018.

Tang XL, Jiang ZX, Li Z, et al. Factors controlling organic matter enrichment in the lower Cambrian Niutitang Formation shale on the eastern shelf margin of the Yangtze block, China. Interpretation. 2017;5(3):1–41. https://doi.org/10.1190/int-2017-0008.1.

Taylor SR, McLennan SM. The continental crust: its composition and evolution. London: Blackwell Scientific Publications; 1985.

Tribovillard N, Riboulleau A, Lyons T, et al. Enhanced trapping of molybdenum by sulfurized marine organic matter of marine origin in Mesozoic limestones and shales. Chem Geol. 2004;213(4):385–401. https://doi.org/10.1016/j.chemgeo.2004.08.011.

Tyrrell T. The relative influences of nitrogen and phosphorus on oceanic primary production. Nature. 1999;400(6744):525–31. https://doi.org/10.1038/22941.

Vorlicek TP, Kahn MD, Kasuya Y, et al. Capture of molybdenum in pyrite-forming sediments: role of ligand-induced reduction by polysulfides. Geochim Cosmochim Acta. 2004;68(3):547–56. https://doi.org/10.1016/S0016-7037(03)00444-7.

Wang J, Li ZX. History of Neoproterozoic rift basins in South China: implications for Rodinia break-up. Precambrian Res. 2003;122(1):141–58. https://doi.org/10.1016/S0301-9268(02)00209-7.

Wang LS, Zou CY, Zheng P, et al. Geochemical evidence of shale gas existed in the Lower Paleozoic Sichuan Basin. Nat Gas Ind. 2009a;29(5):59–62. https://doi.org/10.3787/j.issn.1000-0976.2009.05.011 **(in Chinese)**.

Wang SQ, Chen GS, Dong DZ, et al. Accumulation conditions and exploitation prospect of shale gas in the Lower Paleozoic Sichuan Basin. Nat Gas Ind. 2009b;29(5):51–8. https://doi.org/10.3787/j.issn.1000-0976.2009.05.010 **(in Chinese)**.

Wang J, Chen D, Yan D, et al. Evolution from an anoxic to oxic deep ocean during the Ediacaran–Cambrian transition and implications for bioradiation. Chem Geol. 2012;306–307(2):129–38. https://doi.org/10.1016/j.chemgeo.2012.03.005.

Wang SF, Zou CN, Dong DZ, et al. Multiple controls on the paleoenvironment of the early Cambrian marine black shales in the Sichuan Basin, SW China: geochemical and organic carbon isotopic evidence. Mar Pet Geol. 2015a;66(3):660–72. https://doi.org/10.1016/j.marpetgeo.2015.07.009.

Wang D, Struck U, Ling HF, et al. Marine redox variations and nitrogen cycle of the early Cambrian southern margin of the Yangtze Platform, South China: evidence from nitrogen and organic carbon isotopes. Precambrian Res. 2015b;267(267):209–26. https://doi.org/10.1016/j.precamres.2015.06.009.

Wille M, Nägler TF, Lehmann B, et al. Hydrogen sulphide release to surface waters at the Precambrian/Cambrian boundary. Nature. 2008;453(7196):767–9. https://doi.org/10.1038/nature07072.

Wu CJ, Tuo JC, Zhang MF, et al. Sedimentary and residual gas geochemical characteristics of the lower Cambrian organic-rich shales in Southeastern Chongqing, China. Mar Pet Geol. 2016;75:140–50. https://doi.org/10.1016/j.marpetgeo.2016.04.013.

Xia W, Yu BS, Sun MD. Depositional settings and enrichment mechanism of organic matter of the black shales at the bottom of Niutitang Formation, lower Cambrian in Southeast Chongqing: a case study from Well Yuke 1. Acta Geol Sin. 2015;89(S1):287. https://doi.org/10.2113/econgeo.106.3.511.

Xiao XM, Wei Q, Gai HF, et al. Main controlling factors and enrichment area evaluation of shale gas of the Lower Paleozoic marine strata in South China. Pet Sci. 2015;12(4):573–86. https://doi.org/10.1007/s12182-015-0057-2.

Xu L, Lehmann B, Mao J, et al. Mo isotope and trace element patterns of lower Cambrian black shales in South China: multi-proxy constraints on the paleoenvironment. Chem Geol. 2012;318–319(4):45–59. https://doi.org/10.1016/j.chemgeo.2012.05.016.

Yang RD, Chen ME, Zhao YL. New discovery of bio-fossils at the bottom of the Cambrian of central Guizhou. Prog Nat Sci. 2002;12(2):226–9 **(in Chinese)**.

Yeasmin R, Chen DZ, Fu Y, et al. Climatic-oceanic forcing on the organic accumulation across the shelf during the early Cambrian (Age 2 through 3) in the mid-Upper Yangtze Block, NE Guizhou, South China. J Asian Earth Sci. 2017;134:365–86. https://doi.org/10.1016/j.jseaes.2016.08.019.

Zhang JP, Fan TL, Li J, et al. Characterization of the lower Cambrian shale in the Northwestern Guizhou Province, South China: implications for shale-gas potential. Energy Fuels. 2015;29(10):6383–93. https://doi.org/10.1021/acs.energyfuels.5b01732.

Zhang YY, He ZL, Gao B, et al. Sedimentary environment of the lower Cambrian organic-rich shale and its influence on organic content in the Upper Yangtze. Pet Geol Exp. 2017a;39(2):154–61. https://doi.org/10.11781/sysydz201702154 **(in Chinese)**.

Zhang YY, He ZL, Jiang S, et al. Marine redox stratification during the early Cambrian (ca. 529–509 Ma) and its control on the development of organic-rich shales in Yangtze Platform. Geochem Geophys Geosyst. 2017b;18(6):2354–69. https://doi.org/10.1002/2017GC006864.

Zhang YY, He ZL, Jiang S, et al. Factors affecting shale gas accumulation in overmature shales—case study from lower Cambrian shale in Western Sichuan Basin, South China. Energy Fuels. 2018;32(3):3003–12. https://doi.org/10.1021/acs.energyfuels.7b03544.

Zhu MY, Zhang JM, Steiner M, et al. Sinian-Cambrian stratigraphic framework for shallow-to deep-water environments of the Yangtze Platform: an integrated approach. Prog Nat Sci. 2003;13(12):951–60. https://doi.org/10.1080/10020070312331344710.

Zhu MY, Babcock LE, Peng SC. Advances in Cambrian stratigraphy and paleontology: integrating correlation techniques, paleobiology, taphonomy and paleoenvironmental reconstruction. Palaeoworld. 2006;15(3):217–22. https://doi.org/10.1016/j.palwor.2006.10.016.